Journal of Magnetism and Magnetic Materials 324 (2012) 3709–3715

Contents lists available at SciVerse ScienceDirect

Journal of Magnetism and Magnetic Materials

journal homepage: www.elsevier.com/locate/jmmm

Magnetoelastic phase transitions in the $LuFe_4Ge_2$ and YFe_4Si_2 compounds: A neutron diffraction study

P. Schobinger-Papamantellos [a,*], K.H.J. Buschow [b], J. Rodríguez-Carvajal [c]

[a] Laboratory of Crystallography, ETH-Zurich, 8093 Zürich, Switzerland
[b] Van der Waals-Zeeman Institute, University of Amsterdam, NL-1018 XE, The Netherlands
[c] Institut Laue-Langevin, 156X, 38042 Grenoble Cédex, France

ARTICLE INFO

Article history:
Received 7 May 2012
Available online 12 June 2012

Keywords:
Magnetic structure
Neutron diffraction
Rare earth alloy
Magnetoelastic transition

ABSTRACT

The magnetic structure of the tetragonal antiferromagnetic $LuFe_4Ge_2$ and YFe_4Si_2 compounds has been studied by high resolution neutron and X-ray diffraction above and below the magneto-elastic transition at T_N, T_c=32 K and 76 K, respectively. Below T_N,T_c the tetragonal high temperature (*HT*) phase transforms into the low temperature (*LT*) orthorhombic magnetic phase: $P4_2/mnm$ *(HT)* → *Pnnm* (q=0) (*LT*) with a 2D canted moment arrangement of the Fe moments within the (001) plane with the magnetic space group $P\frac{2_1}{n'}\frac{2_1}{n'}\frac{2_1}{m'}(Sh_{58}^{399})$. The Fe magnetic moment value is highly reduced in both compounds due to the presence of geometrical and exchange frustration relating to the underlying crystal structure comprising columns of Fe tetrahedra expanding along the *c* direction with antiferromagnetic interactions. The magnetic refinements were perturbed by the presence of partly unidentified impurity phases mainly in YFe_4Si_2.

1. Introduction

The $LuFe_4Ge_2$ and YFe_4Si_2 compounds crystallise with the tetragonal $ZrFe_4Si_2$-type of structure (space group, $P4_2/mnm$ (no. 136), $a \approx 7.004$ Å, $c \approx 3.755$ Å, $Z \approx 2$) [1]. In this structure type the Fe atoms occupy the *8i* symmetry site at (0.092, 0.346, 0) forming slightly distorted tetrahedra columns along the direction *c*. The Ge or Si atoms occupy the *4g* site at (0.221, −0.221, 0) and the Lu, Y atoms occupy the *2b* site at (0, 0, 1/2). According to a recent magnetic and specific heat study [2], $LuFe_4Ge_2$ and YFe_4Si_2 order antiferromagnetically at 32 K and 76 K respectively like all the isomorphs studied by us using neutron and X-ray diffraction [3–12]. According to the same study the latter compound undergoes a second transition below 56 K.

Our previous powder neutron diffraction studies on the isomorphous compounds RFe_4Ge_2 (R=Dy, Ho, Er, Tm and Y) found a puzzling non-uniform behaviour across the series when *R* is a magnetic atom [4–12]. Without exception, the magnetic ordering is accompanied by symmetry reduction and numerous magnetoelastic first-order transitions with *T* relating to competing interactions of the two magnetic systems. The transition path depends strongly on the nature of the magnetic *R* atom. Until now, two low temperature (*LT*) orthorhombic crystal structures were found, either *Cmmm* (no. 65) or *Pnnm* (no. 58). Both *LT* structure types harbour complex magnetic structures ranging from long period structures to incommensurate magnetic structures, and numerous transitions occur among them. In some cases the two *LT* phases coexist while their relative amounts vary with temperature.

A first-order transition was also found when *R* is a non-magnetic atom, as in the YFe_4Ge_2 compound [3]. Here magnetic ordering occurs below 43.5 K, simultaneously with a structural transition from tetragonal $P4_2/mnm$ to orthorhombic *Pnnm* symmetry. This means that in contrast to the T-phase diagram(s) of the compounds in which *R* is a magnetic rare earth, for the YFe_4Ge_2 compound there are no two coexisting structures in the *LT* range ($T < T_N$, T_c) but exclusively a structure of *Pnnm* symmetry. Its magnetic structure is canted and commensurate with (q=0). The first-order transition can therefore be characterized by the sequence $P4_2/mnm$ (T_N, T_c)=43.5 K⇒*Pnnm* (q=0). The calculated Fe ordered magnetic moment value at 1.5 K is fairly small and equals 0.63(4) μ_B/Fe atom, in agreement with the Fe moments found in the compounds with R=Dy, Ho, Er, Tm [4–12]. This suggests that the primary order parameter of this transition relates to the behaviour of the Fe sublattice.

In the present paper we have extended our previous studies on the magnetoelastic transitions in RFe_4X_2 (R=rare earth, X= Ge, Si) compounds with $LuFe_4Ge_2$ and YFe_4Si_2 in order to clarify the role of the iron sublattice in this type of transitions more clearly.

2. Experimental and results

Neutron diffraction patterns of the $LuFe_4Ge_2$ and YFe_4Si_2 compounds were collected with the high resolution (*HR*) D2B

* Corresponding author. Tel.: +41 44 632 3773; fax: +41 44 632 1133.
E-mail addresses: Schobinger@mat.ethz.ch (P. Schobinger-Papamantellos), buschow@gmail.com (K.H.J. Buschow).

0304-8853/$ - see front matter © 2012 Elsevier B.V. All rights reserved.
http://dx.doi.org/10.1016/j.jmmm.2012.05.058

diffractometer (λ=1.5941 Å, 2θ=3–160°, step increment of 0.05°) for various temperatures above and below T_N at 60, 30 and 1.5 K for $LuFe_4Ge_2$ and at 100, 60 and 5 K for YFe_4Si_2. Room temperature data of YFe_4Si_2 were also collected with the *HR* D1A diffractometer (λ=1.914 Å, 2θ=3–160°, step increment of 0.05°) and the BM16 X-ray diffractometer (λ=0.40578 Å, 2θ=4–30°) at the ESRF in Grenoble. The X-ray refinements did not converge as the YFe_4Si_2 sample contains a considerable amount of impurity phases. A search using the X-pert data bank led to the identification of the Y_2Fe_{17}, Fe_2Si and α-Fe phases. However, the problem was not fully solved due to the presence of additional unidentified impurity peaks. Apparently the Y–Fe–Si phase diagram is not yet fully explored. Therefore we will show the refined D2B 100 K paramagnetic neutron data of YFe_4Si_2 and only selected parts of the *LT* data regarding the transition. The $LuFe_4Ge_2$ sample contains only minor amounts of foreign phase(s), included successfully in

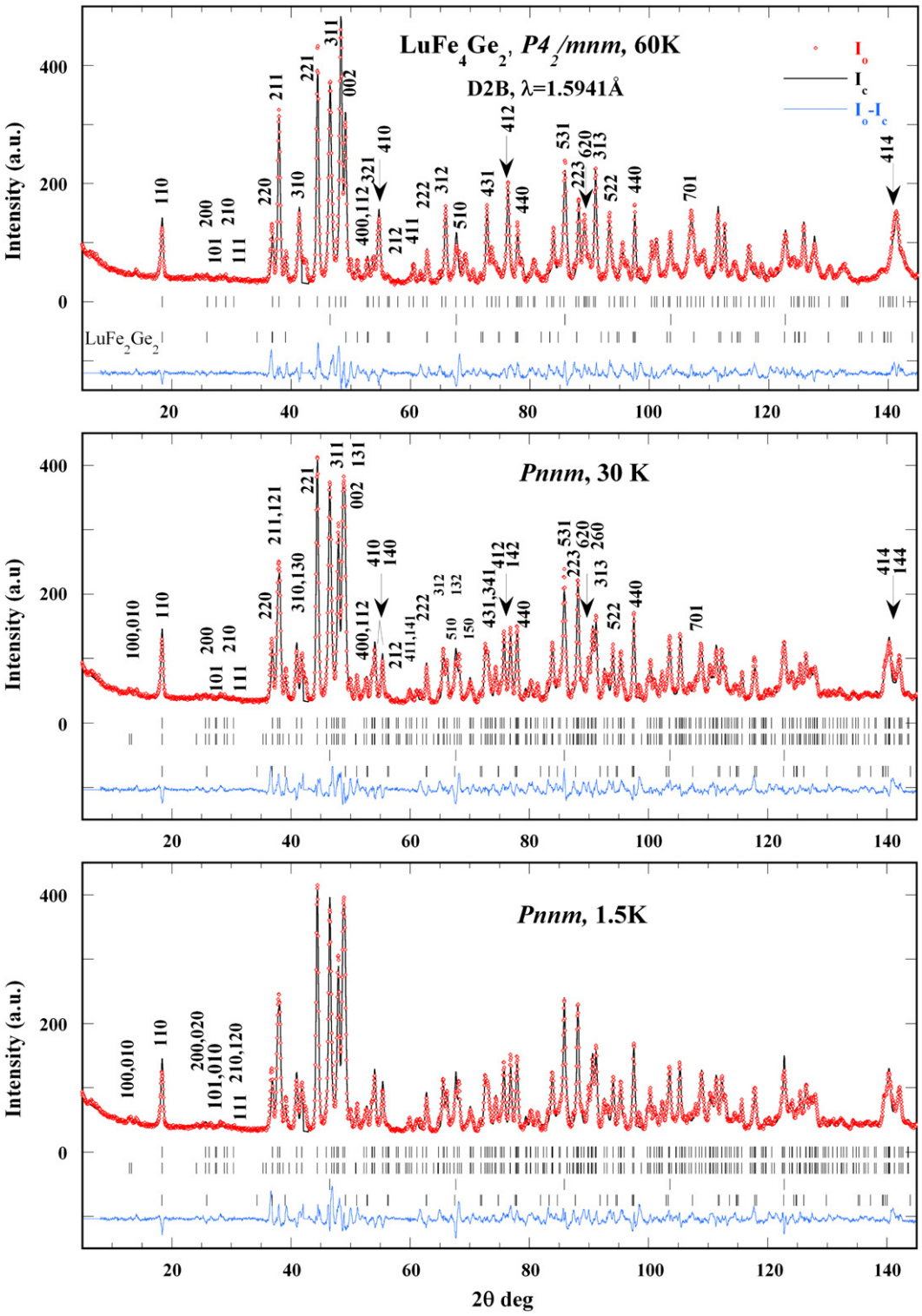

Fig. 1. Observed and calculated neutron patterns of $LuFe_4Ge_2$: (a) in the paramagnetic state at 60 K (tetragonal symmetry), (b) in the magnetically ordered state at 30 K just below T_N, T_c= 32 K (orthorhombic symmetry and (c) at 1.5 K. The sample contains 13.4% $Y_2Fe_2Ge_2$, and 8% a-Fe impurity phases.

Table 1
Refined structural parameters of the $LuFe_4Ge_2$ and YFe_4Si_2 compounds from HR neutron powder data (a) in the paramagnetic state (tetragonal phase $P4_2/mnm$) at 60 K and 100 K respectively. For $LuFe_4Ge_2$ we also give results in the magnetically ordered state at 30 K and 1.5 K. R_B, R_m, R_{wp} and $R_{exp\%}$ are the Bragg, the magnetic, the weighted profile and the expected reliability factors respectively.

$P4_2/mnm$	$LuFe_4Ge_2$ 60 K			YFe_4Si_2 100 K		*Pnnm*	$LuFe_4Ge_2$ 30 K		$LuFe_4Ge_2$ 1.5 K	
Atom	*x*	*y*	*z*	*x*	*y*	Atom	*x*	*y*	*x*	*y*
Lu(Y): *2b*	0	0	½			Lu:*2b*	0	0	0	0
Fe : *8i*	0.0907_3	0.3533_3	0	0.0914_6	0.3496_5	Fe1 at *4g:*	0.0961_4	0.3537_4	0.0961_4	0.3533_4
	0.3533_3	0.0907_3	0	0.3533_3	0.0907_3	Fe2 at *4g*	0.3537_4	0.0869_4	0.3532_4	0.0868_4
Ge (Si): *4g*	0.2160_3	-0.2160_3	0	0.213_1	-0.213_1	Ge at *4g:*	0.2110_4	-0.2203_5	0.2112_4	-0.2195_5
a, *b* (Å)	7.1986_3	7.1986_3		7.1792_4	7.1792_4		7.2841_3, 7.1091_3,	7.2884_3, 7.1048_3		
a/*b*	1			1			1.025	1.026		
c (Å)	3.8655_1			3.7767_3			3.8687_1		3.8689_1	
B_{ov} (Å^2)	0.07_5			0.06_5			0.28_6		0.29_5	
R_B, R_m, R_{wp}, %	4.74, -, 16.2,			10, -, 28,			6, 21, 17		5.7, 19.7, 16.8	
R exp%, χ^2,	5.17, 9.8			7.4, 14.7			5, 11.8		4.69, 12.8	

Table 2
Refined magnetic moment components of $LuFe_4Ge_2$ from neutron *HR* data in the magnetically ordered state. The *x*, *y* parameters are from Table 1.

Atom/site	*x*	*y*	*z*	μ_x (μ_B)	μ_y (μ_B)	μ_T (μ_B)
nnm	15 K					
Fe1: *4g (x,y,0)*	0.0962_4	0.3533_4	0	0.4_1	-0.2_1	0.44_7
Fe2: *4g* 4g*(x,y,0)*	0.3532_4	0.0868_4	0	0.2_1	-0.4_1	0.44_7
Pnnm	30 K					
Fe1: *4g (x,y,0)*	0.0961_4	0.3537_4	0	0.32_9	-0.2_1	0.38_8
Fe2: *4g* 4g*(x,y,0)*	0.3537_4	0.0869_4	0	-0.2_1	0.32_9	0.38_8

the data analysis that has been made with the *FullProf Suite* of programs [13]. The plots of the magnetic structure were made with the programme *FullProf Studio* [14] incorporated in [13].

2.1. $LuFe_4Ge_2$ HT paramagnetic state

The 60 K refinement of the $LuFe_4Ge_2$ tetragonal ($P4_2/nmn$) compound in the paramagnetic state (D2B, *HR* instrument) has shown that the sample contains 9% $LuFe_2Ge_2$ (tetragonal) and 13.3% α-Fe that were included in the calculations. Unexplained non-overlapping peaks, as the peak at $2\theta=42.5°$, were excluded from the refinement. However, the difference diagram in Fig. 1 indicates the presence of small amount of unknown impurity with overlapping peaks. The *R*-factors ($R_B=4.74\%$, $R_{wp}=16\%$) of the refinement given in Table 1 are satisfactory and confirm the tetragonal $ZrFe_4Si_2$ type of structure.

2.2. $LuFe_4Ge_2$ first-order ferroelastic transition

One observes remarkable changes in the peak topology when comparing the paramagnetic 60 K pattern to the 30 K pattern obtained just below the magnetoelastic transition at T_N, $T_c=32$ K and to the pattern obtained at the lowest measuring temperature, 1.5 K (Fig. 1).

The structural transition is clearly seen following the enlargement and splitting of several selected *hklt* tetragonal reflections going from 60 K to lower temperatures. The largest splitting occurs for the *hklt* reflections with the largest difference $h-k$ as (410), (412), (620) marked by arrows in Fig. 1. This is in contrast to the observations of the *hhlt* reflections that remain unchanged. These facts indicate that the ratio $(a/b)_t \neq 1$ deviates from 1 and therefore the tetragonal symmetry tends towards orthorhombic.

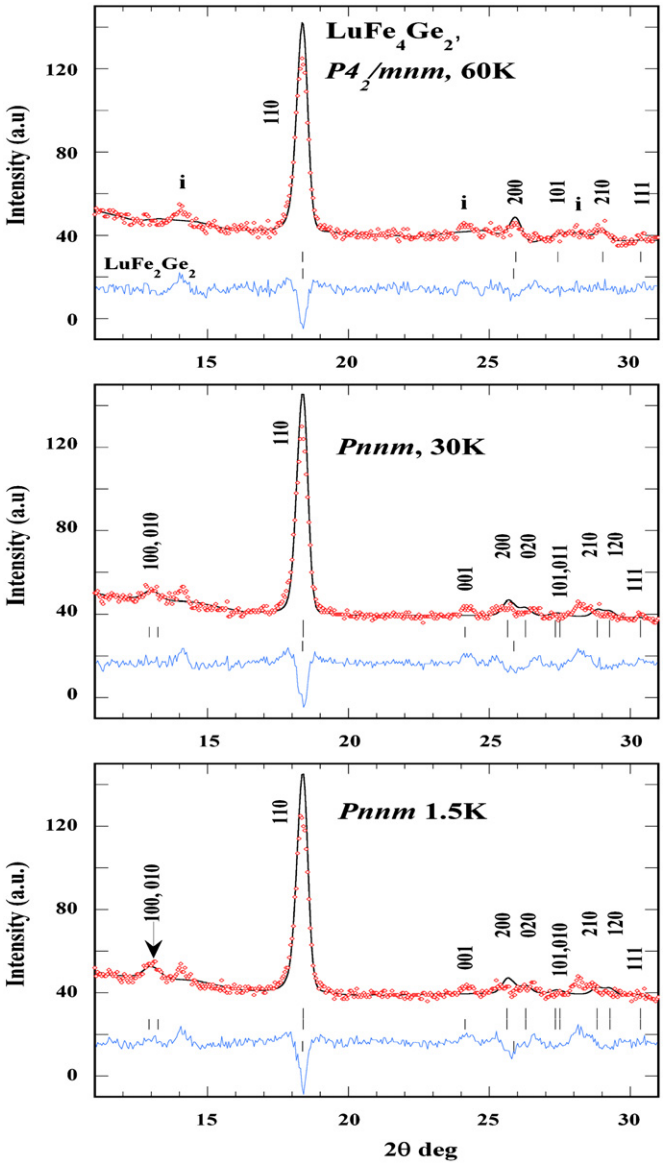

Fig. 2. The low angle part of observed and calculated neutron patterns of $LuFe_4Ge_2$ at 60 K (paramagnetic) and 30 K and 1.5 K (magnetic state). The only resolved weak 100/010 magnetic line at $2\theta=12.9°$ becomes visible already at 30 K and increases slightly down to 1.5 K. (i) denotes impurity lines.

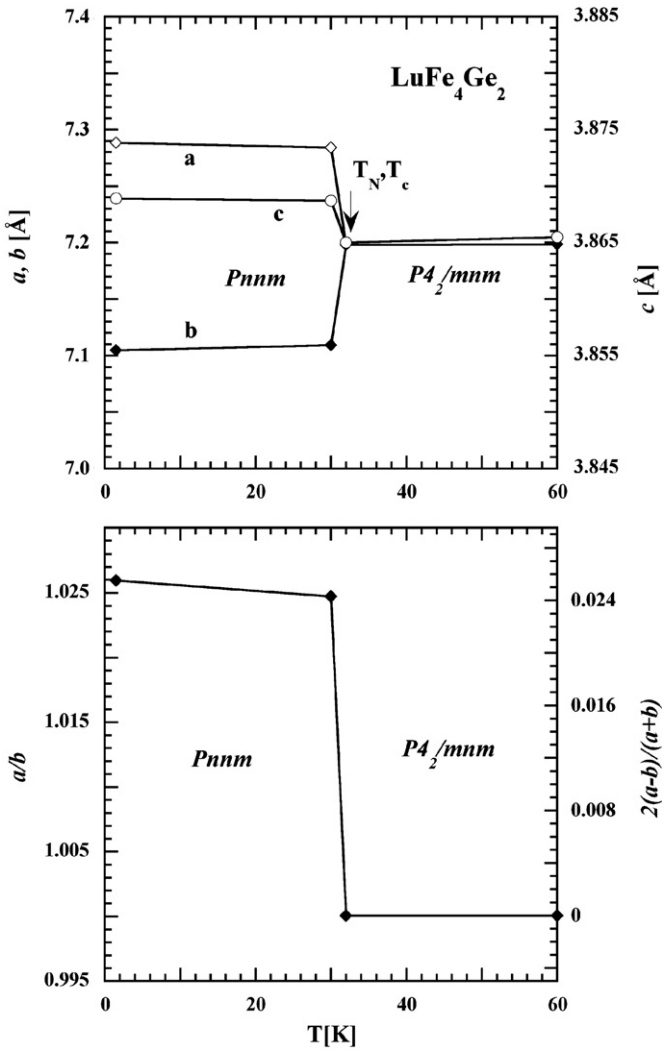

Fig. 3. Temperature dependence of (a) the lattice parameters (top part) (b) of the (a/b) ratio and the strain parameter $\varepsilon s\ 2|(a-b)/(a+b)|exx-eyy|$ of $LuFe_4Ge_2$ (bottom part).

The only orthorhombic subgroup of order 2 of $P4_2/mnm$ that fulfils this condition is *Pnnm*. Results for the *LT* refinements in the *Pnnm* space group are summarised in Tables 1 and 2 for 1.5 and 30 K respectively.

Similar to the YFe_4Ge_2 findings [3] one may assume the simultaneous occurrence of magnetic order and a structural transition from tetragonal to orthorhombic: $P4_2/mnm$ (T_c,T_N)→ *Pnnm*. The partly overlapping weak magnetic contributions not visible in Fig. 1 are better shown on a larger scale in the low angle 2θ range in Fig. 2. In fact the only resolved very weak magnetic reflection is around 2θ 12.7° at the position(s) of the (100/010) reflections, forbidden by the space group that suggest that the magnetic and crystal cell have the same size ($q=0$). This peak becomes visible already at 30 K just below T_N, T_c and increases only slightly down to 1.5 K. The low intensity of this peak suggests strongly reduced Fe moments. This is most likely due to antiferromagnetic interaction of the Fe moments located at the corners of a tetrahedral geometric arrangement along the c direction that lead to frustration. The peak at the (001) position ($2\theta=24.2°$) most likely pertains to an impurity as it exists already at 60 K.

The *LT* structural parameters at 30 K and 1.5 K and the ratio $a/b=1.025$ are identical within the 3 s limit. As shown in Fig. 3 the transition is associated with a jump of the lattice parameters, of the a/b ratio and of the tensile strain $e_1=e_{xx}-e_{yy}=\ \Delta a/a--\Delta b/b=2|(a-b)/(a+b)|$. The strong change of 2.5×10^{-2} of the tensile strain suggests a first-order character for this ferroelastic transition from tetragonal to orthorhombic (Fig. 4) symmetry.

In the *Pnnm* space group with the wave vector $q=0$, the Fe site splits into two sites (see Fig. 3). Orbit Fe1 (orange colour) comprises the atoms Fe1: 1–4 and orbit 2 (green) comprises atoms Fe2: 1'–4'. The calculated atomic displacement Δx, Δy between 30 K and the tetragonal 60 K tetragonal x, y values are given in Table 3. The displacement field suggests that the main contribution ($e_{xx}-e_{yy}$) to the macroscopic strain that triggers the symmetry lowering is the shifting of the Fe atoms shown by arrows in Fig. 4. From this figure it becomes obvious that the symmetry breaking is connected with the fact that orbit Fe1 has mainly $\pm\Delta x$ and orbit Fe2 mainly $\pm\Delta y$ components that induce the symmetry-breaking tensile strains. The antiparallel displacements along the x and y directions of the Fe1 and Fe2

Table 3
The splitting of the *8i* Fe site in transition $P4_2/mnm$ (no 136) → *Pnnm* (58) into two 4*g* sites observed in $LuFe_4Ge_2$ and YFe_4Si_2 below T_N. Δx, Δy are the atomic displacements and $\Delta x/x=e_{xx}$, $\Delta y/y=e_{yy}$ are the strain components between 60 K > T_N and $T=30$ K > T_N observed in $LuFe_4Ge_2$ ($T_N=32$ K).

$P4_2/mnm$ Atom site		x	y	z	*Pmnn* Atom site		x	y	z	$LuFe_4Ge_2$ 30 K Δx $\Delta x/x$	Δy $\Delta y/y$
Fe :*8i*	1	x	y	0	Fe1:*4g*	1	x	y	0	− 0.0054 0.0595	− 0.0004 0.0011
	2	$-x$	$-y$	0		2	$-x$	$-y$		+ 0.0054 0.0595	+0.0004 0.0011
	3	$-y+1/2$,	$x+1/2$	1/2		3	$-x+1/2$,	$y+1/2$	1/2	+ 0.0054 0.0595	− 0.0004 0.0011
	4	$y+1/2$	$-x+1/2$	1/2		4	$x+1/2$			− 0.0054 0.0595	+0.0004 0.0011
	5	$-x+1/2$	$y+1/2$	1/2	Fe_2:*4g*	1'	y			− 0.0038	− 0.0004
	6	$x+1/2$	$-y+1/2$	1/2		2'	$-y$	$-x$ $-y+1/2$	0 1/2	+ 0.0004	+0.0038
	7	y	x	0		3'	$-y+½$	$x+1/2$	1/2 0	+ 0.0004 0.0011	− 0.0038 0.0414
	8	$-y$	$-x$	0		4'	$y+1/2$	$-x+1/2$	1/2 0	− 0.0004 0.0011	+ 0.0038 0.0414
Ge : *4g*	1	x	$-x$	0		1	x	$-y$	0	+ 0.005 0.023	− 0.004 0.018
	2	$-x$	x	0		2	$-x$	y	0	− 0.005 0.023	+ 0.004 0.018
	3	$-x+1/2$	$x+1/2$	½		3	$x+1/2$	$y+1/2$	1/2	+ 0.005 0.023	− 0.004 0.018
	4	$-x+1/2$	$-x+1/2$	1/2		4	$-x+1/2$	$-y+1/2$	1/2	− 0.005 0.023	+ 0.004 0.018

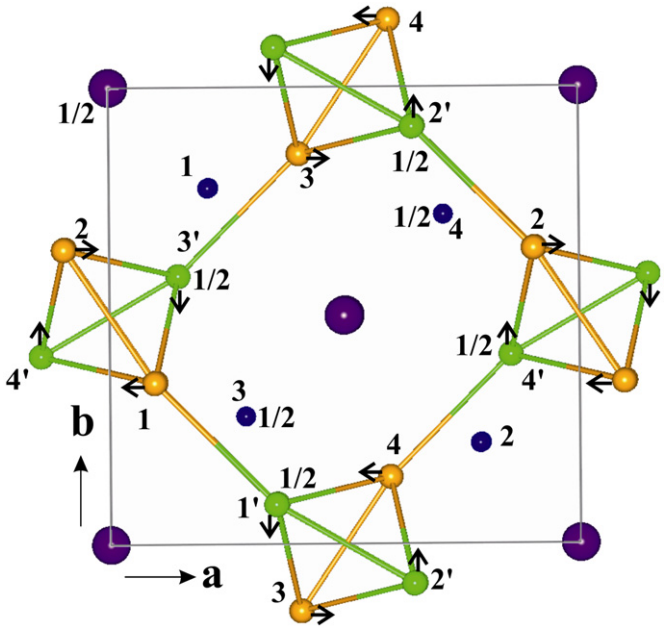

Fig. 4. The Fe displacive field mechanism, in the transition $P42/mnm \rightarrow Pnnm$ in the $LuFe_4Ge_2$ (001) plane. The displacive field of the Fe atoms between 60 K and 30 K is displayed by arrows. The two Fe orbits have only either a $\pm\Delta x$ orbit 1 (atoms 1–4) or a $\pm\Delta y$ orbit 2 (atoms 1'–4'). The labeling of the atoms is given in Table 3.

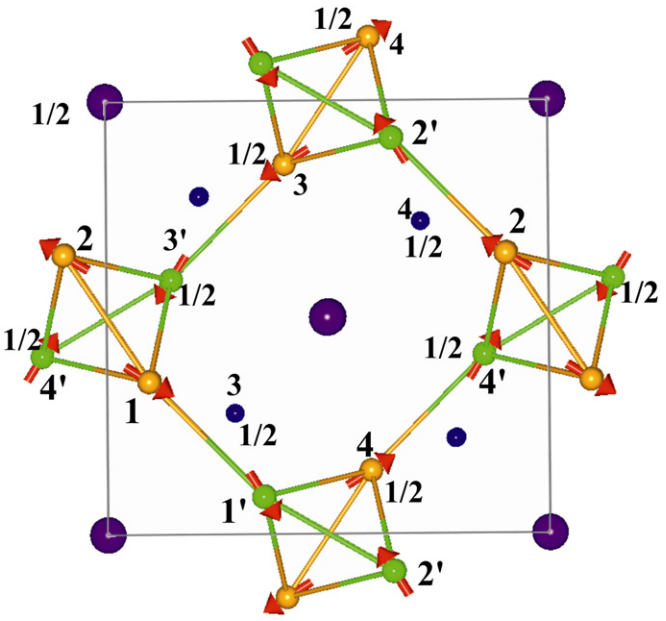

Fig. 5. Schematic representation of the $LuFe_4Ge_2$ magnetic structure along the [001] direction, at 1.5 K. The labels 1–4 and 1'–4' denote the atoms of the Fe1 and Fe2 orbits respectively.

Table 4
Fe–Fe interatomic distances in (Å) in the distorted compact Fe tetrahedra for various temperatures in $LuFe_4Ge_2$.

Distance	$P4_2/mnm$	$Pnnm$	
	60 K	30 K	1.5 K
Fe1–Fe3'	2.617(2)	2.666(4)	2.663(4)
Fe1–Fe4'	2.617(2)	2.651(3)	2.655(3)
Fe1–Fe2	2.495(3)	2.576(3)	2.577(3)
Fe4'–Fe3'	2.495(3)	2.505(4)	2.511(4)

The atoms of the two Fe sublattices correspond to those of Figs. 4 and 5.

orbits respectively lead to dilatation along the *a*-axis and to contraction along the *b* axis. The role of the Ge atomic shift is considered of minor importance as it is oblique to both *a* and *b* axes. Table 4 displays the changes of the shorter Fe-Fe interatomic distances below the T_N, T_c transition.

2.3. Magnetic structure of $LuFe_4Ge_2$

Because of the very weak magnetic intensity, the moments of the two Fe orbits were constrained to the same value in the refinements and the (001) plane model was imposed by symmetry considerations. The Fe atoms of the 4*g* site located at the mirror plane m_z at $z=(0, 0, 1/4)$ may have either a single component along the *c* direction for an m_z mirror plane or two moment components m_x, m_y for an antimirror plane $m_{z'}$. The best fit led to the latter choice with a planar (m_x, m_y, 0) magnetic moment arrangement. The ordered Fe moment value is 0.44(7) μ_B/atom. The moment components of the two orbits were constrained so that the m_x and m_y components of orbit Fe1 are equal to the $m_{y'}$ and $m_{x'}$ components of Fe2, respectively. This reflects the tendency to restore the lost 4_2 tetragonal symmetry. The magnetic space group is $P\frac{2_1}{n'}\frac{2_1}{n'}\frac{2_1}{m'}(Sh_{58}^{399})$ or 58.7.477 according to the classification of [15]. The total structure associated with the wave vector ($q=0$) can be considered as a planar antiferromagnetic arrangement similar to YFe_4Ge_2 with eight Fe sublattices (1–4 and 1'–4') shown in Fig. 5. This arrangement involves isotropic and anisotropic exchange interactions. The calculated magnetic moment components between 30 and 1.5 K (Table 2) do not display strong changes. This also suggests a first-order character for the magnetic transition with an abrupt intensity change at T_N, $T_c=32$ K.

2.4. YFe_4Si_2

The refinement of the 100 K YFe_4Si_2 (tetragonal) high resolution neutron powder data (D2B instrument), in the paramagnetic state, shows the presence of the hexagonal Fe_2Y_{17} (37.8%) and (5.8%) of Fe_2Si impurity phases. As already mentioned, unexplained additional peaks led to a rather high $R_{wp}=28\%$ in the refinement (see difference diagram in Fig. 6). despite the sample quality, the 60 K data below the reported magnetoelastic transition T_N, $T_c=$ 76 K [1] confirm the *LT* orthorhombic structure. Most likely the transition from tetragonal to orthorhombic occurs simultaneously with the onset of magnetic order, similarly to the YFe_4Ge_2 compound [2]: $P4_2/mnm$ T_c, $T_N \rightarrow Pnnm$. We restrict ourselves to show only characteristic 2θ ranges with regard to the magnetoelastic transition.

The left part of Fig. 7 displays the changes in the peak topology as the increasing enlargement or splitting of the tetragonal *hkl* reflections (210) and (310) on cooling from the paramagnetic state at 100 K across T_N, $T_c=76$–60 K and down to 5 K. The right part of Fig. 7 considers the expected (100/010) magnetic reflections associated with the wave vector $q=0$ in the *Pnnm* space group, similar to YFe_4Ge_2. It shows that the intensity contribution at the position of the expected magnetic reflection is almost not distinguishable from the background, suggesting a quenching of the Fe moments due to antiferromagnetic interaction in the tetrahedral arrangement. Therefore the moment value cannot be estimated by neutron diffraction. The almost negligible intensity of this peak reached saturation already at 60 K.

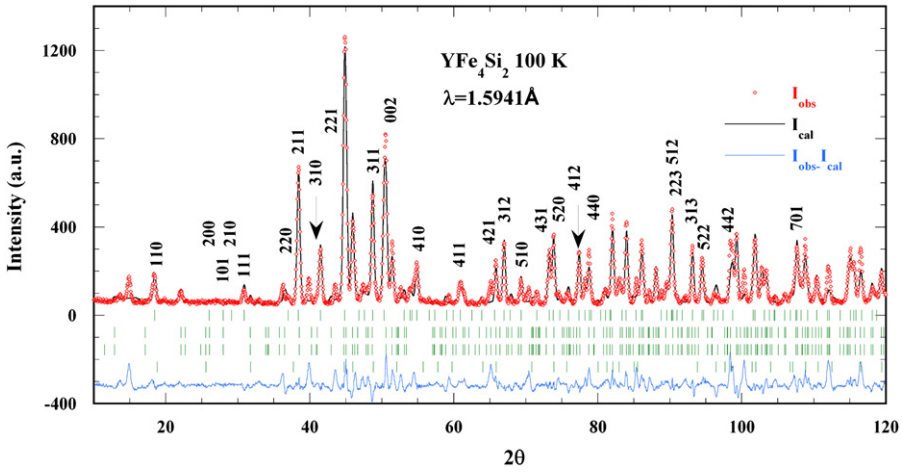

Fig. 6. Observed and calculated neutron patterns of YFe_4Si_2, in the paramagnetic state at 100 K (tetragonal symmetry). The sample contains 38% Y_2Fe_{17}, 5.8% Fe_2Si and further unidentified impurity phases (see peaks in the difference diagram).

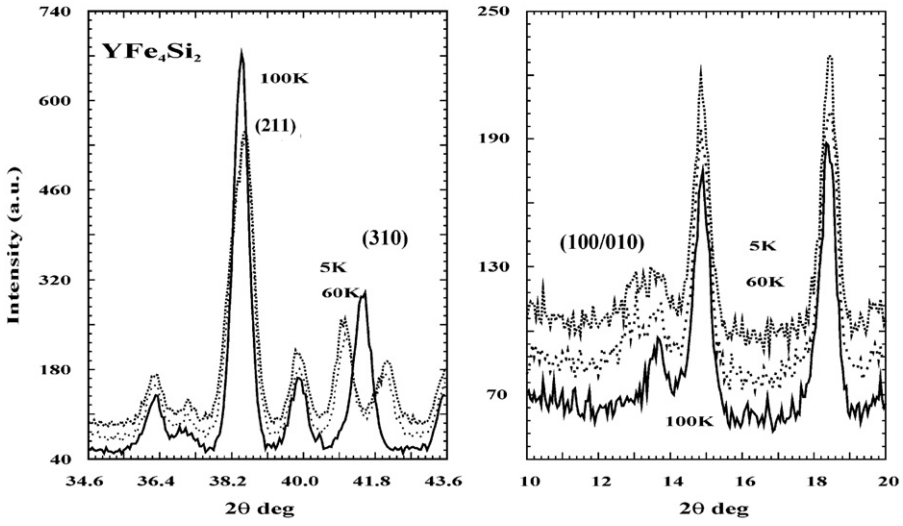

Fig. 7. The splitting of the tetragonal reflection (310)$t\rightarrow$(310/130)o in the *Pnnm* space group (left part). The only resolved magnetic reflection (100/010) in YFe_4Si_2 ($\lambda=$ 1.5941 Å) (right part).

3. Concluding remarks

The investigated tetragonal compounds $LuFe_4Ge_2$ and YFe_4Si_2 order antiferromagnetically, like the previously examined isomorphic YFe_4Ge_2 compound. In all these cases the magnetic ordering is exclusively due to the Fe moments and is accompanied by a first-order phase transition from tetragonal to orthorhombic symmetry $P4_2/mnm \rightarrow Pnnm$. It is interesting to note that this type of phase transition apparently is independent of the changes in lattice parameters (and the concomitant Fe–Fe distances) which increase substantially in the sequence $YFe_4Si_2 > LuFe_4Ge_2 > YFe_4Ge_2$. It is equally interesting to note that this type of phase transition survives any changes in exchange interaction between the Fe moments, bearing in mind that the magnetic ordering temperature more than doubles when passing through the mentioned sequence.

When comparing these results with the previously investigated RFe_4Ge_2 compounds where R is a magnetic rare earth element (R=Dy; Ho, Er, Tm) we note that the magnetic ordering is accompanied by a first-order phase transition from tetragonal to orthorhombic symmetry $P4_2/mnm \rightarrow Pnnm$ only in the case of the $ErFe_4Ge_2$ and $TmFe_4Ge_2$ compounds (although here a more complicated situation exists as the phase diagram comprises two competing *LT* phases). However, in the Dy and Ho compounds the *LT* phase is different as its crystal structure belongs exclusively to the *Cmmm* space group. The results mentioned above show that this difference in behaviour between the two groups does not originate from size effects but rather has to be related to the differences in the rare earth moment configuration. When thinking in purely (crystal) structural arguments, such preponderant role of the rare earth moment configuration is rather unexpected. We showed, however, that in the RFe_4Ge_2 compounds strong magneto-elastic couplings prevail and then the sign difference in the first-order Stevens factor between Dy,Ho ($\alpha_J<0$) and Er,Tm($\alpha_J>0$) can become of influence.

References

[1] Ya.P. Yarmoluk, L.A. Lysenko, E.I. Gladyshevski, Dopovidi Natsional'noi Akademii nauk Ukrainy RSR, Series A. 37 (1975) 279.
[2] G. Geibel et al. (submitted for publication).
[3] P. Schobinger-Papamantellos, J. Rodríguez-Carvajal, G. André, C.H. de Groot, F.R. de Boer, K.H.J. Buschow, Journal of Magnetism and Magnetic Materials 191 (1999) 261.
[4] P. Schobinger-Papamantellos, J. Rodríguez-Carvajal, K.H.J. Buschow, E. Dooryhee, A.N. Fitch, Journal of Magnetism and Magnetic Materials 300 (2006) 315–332.
[5] P. Schobinger-Papamantellos, J. Rodríguez-Carvajal, G. André, K.H.J. Buschow, Journal of Magnetism and Magnetic Material 300 (2006) 333–350.

[6] P. Schobinger-Papamantellos, J. Rodríguez-Carvajal, K.H.J. Buschow, E. Dooryhee, A.N. Fitch., Journal of Magnetism and Magnetic Materials 250 (2002) 225–240.
[7] P. Schobinger Papamantellos, J. Rodrìguez-Carvajal, K.H.J. Buschow, Journal of Magnetism and Magnetic Materials 280 (2004) 119–142.
[8] P. Schobinger-Papamantellos, J. Rodríguez-Carvajal, G. André, C.H. de Groot, F.R. de Boer, K.H.J. Buschow, Journal of Magnetism and Magnetic Materials 191 (1999) 261.
[9] P. Schobinger-Papamantellos, J. Rodríguez-Carvajal, K.H.J. Buschow, E. Dooryhee, A.N. Fitch, Journal of Magnetism and Magnetic Materials 210 (2000) 121.
[10] P. Schobinger-Papamantellos, Ted Janssen, **Z** Kristallog**r** 221 (2006) 732.
[11] P. Schobinger-Papamantellos, J. Rodríguez-Carvajal, K.H.J. Buschow, Journal of Magnetism and Magnetic Materials 310 (2007) 63.
[12] P. Schobinger-Papamantellos, K.H.J. Buschow, J. Rodríguez-Carvajal, submitted for publication.
[13] J. Rodríguez-Carvajal, Physica B 192 (1993) 55. The programs of the FullProf Suite and their corresponding documentation can be obtained from the Web at 〈http://www.ill.eu/sites/fullprof/〉.
[14] L.C. Chapon, J. Rodríguez-Carvajal , FullProf Studio is a program of the FullProf Suite that is freely available in the site given in Ref. [13].
[15] D.B. Litvin, Acta Crystallographica A64 (2008) 419.